

# ***Arabidopsis thaliana* telomeric DNA-binding protein 1 is required for telomere length homeostasis and its Myb-extension domain stabilizes plant telomeric DNA binding**

Moo Gak Hwang and Myeon Haeng Cho\*

Department of Biology, Yonsei University, Seoul 120-749, Republic of Korea

Received August 4, 2006; Revised November 3, 2006; Accepted January 10, 2007

## **ABSTRACT**

**Telomeres are specific protein–DNA complexes that protect the ends of eukaryotic chromosomes from fusion and degradation and are maintained by a specialized mechanism exerted by telomerase and telomere-binding proteins (TBPs), which are evolutionarily conserved. AtTBP1 is an *Arabidopsis thaliana* protein that binds plant telomeric DNA *in vitro*. Here, we demonstrated that lack of AtTBP1 results in a deregulation of telomere length control, with mutant telomeres expanding steadily by the fourth generation. DNA-binding studies with mutant AtTBP1 proteins showed that the Myb-extension domain of AtTBP1 is required for binding to plant telomeric DNA. Our results suggest that AtTBP1 is involved in the telomere length mechanism in *A. thaliana* and that the Myb-extension domain of AtTBP1 may stabilize plant telomeric DNA binding.**

## **INTRODUCTION**

Eukaryotic telomeres are maintained by several telomeric factors, including telomerase, shelterin subunits (TRF1, TRF2, TIN2, Rap1, TPP1 and POT1) and non-shelterin proteins (Mre11/Rad50/Nbs1, ERCC1/XPF, WRN, BLM, DNA-PK, Tankyrases and Rad51D) (1). The typical shelterin components, TRF1 and TRF2, recognize telomeric DNA, have the capacity to regulate t-loop structures, and can be involved in the canonical DNA damage response (1,2). The *in vivo* dominant inhibition studies suggest that the main function of TRF1 is to negatively regulate telomere length (3) and that of TRF2 is to protect chromosome ends (4). In mouse embryonic cells, a conditional null mutation in TRF1 induces growth defects and chromosomal instability (5). Deletion of TRF2 results in extensive telomere fusions and activates

the DNA damage response machinery without detectable degradation of the telomeric DNA (6).

In contrast to mammals, *Arabidopsis thaliana* displays a remarkable tolerance to telomere dysfunction and chromosome instability (7,8). This makes *A. thaliana* a useful system to investigate the roles of shelterin genes in telomere biology by studying lines containing multiple mutations. For example, the disruption of *AtTERT* gene leads to telomere shortening and the symptom of developmental defects in the sixth generation of the mutant (9). *AtRad50* mutant cells present a dramatic loss of telomeric DNA and cell death (10). In contrast, *A. thaliana* mutants lacking *Ku70*, *Ku80* and *MRE11* display increased telomere length (11–13). Using activation-tagged line screening method, Ren *et al.* characterized a novel zinc-finger protein, telomerase activator 1, which induces telomerase in leaves (14). However, this activity does not increase telomere length. This result implies that access to the telomeres by telomerase is regulated by shelterin proteins. Thus shelterin is more critical regulator in telomere homeostasis.

Although several non-shelterin proteins from plants have been characterized, the physiological functions of the *A. thaliana* double-stranded TBPs have not previously been assessed. Several *A. thaliana* *AtTBP* genes have been identified, and these genes encode proteins that specifically bind to plant telomeric DNA *in vitro* (15,16). These proteins are similar in structure to the mammalian TRFs as they harbor a single Myb telomeric DNA-binding domain in their C-terminus (16). Here, we investigate the role of *A. thaliana* telomeric DNA-binding protein 1 (*AtTBP1*) in telomere maintenance and describe the consequences of an *AtTBP1* deficiency in *A. thaliana*. In the mouse, inactivation of the shelterin (*mTRF1* or *mTIN2* genes) results in embryonic lethality, and this phenotype is not due to unregulated telomeric function (17,18). In contrast, we found that mutant *AtTBP1* plants were viable and that a lack of this gene resulted in a

\*To whom correspondence should be addressed. Tel: +82 2 2123 4460; Fax: +82 2 312 5657; Email: mhcho@yonsei.ac.kr

deregulation of telomere length control, with mutant telomeres expanding steadily by the fourth generation.

## MATERIALS AND METHODS

### Plant material and growth conditions

*Arabidopsis thaliana* plants (ecotype Wassilewskija) were cultivated at 22°C in a growth chamber under a 16/8 h light/dark photoperiod. *Arabidopsis* seeds were surface sterilized in 5% bleach solution and plated on solid 1X Murashige and Skoog (MS) medium or transferred to soil.

### Mutant identification

We screened the Institut National de la Recherche Agronomique Versailles (INRAV) *Arabidopsis* T-DNA insertion collection, using the flanking insertion site FLAG sequence database (19), and identified a putative mutant plant (FST 072C05) with a T-DNA insertion in the *AtTBP1* gene. The progeny of plants heterozygous for a T-DNA insertion into the *AtTBP1* gene were genotyped by PCR, using the primers TBP1-KO-F (5'-CTTCTCCA GCGTTAGAGACTGGAAT-3'), TBP1-KO-R (5'-CCAT GGTCTACCACCAAATTACAT-3') and L1 (T-DNA left border) (5'-CTACAAATTGCCTTTTCTTATCG AC3'). A 997-bp product was generated from the wild-type allele and a 593-bp product from the disrupted allele. For segregation analysis and for the selection of plants heterozygous or homozygous for the T-DNA insertion, germination medium was supplemented with 10 µg/ml 5-phosphoribothricine. Plants homozygous for the *AtTBP1* disruption (referred to as G1) were self-pollinated to obtain subsequent generations. For the DNA blots, 10 µg total DNA, isolated using a standard method (20), were digested overnight with EcoRI or HindIII. The probe used on the blot was a 1.5-kb GUS fragment, labeled with [ $\alpha$ -<sup>32</sup>P]dCTP.

### Expression analysis of *AtTBP1* mRNA

Fifteen micrograms of total RNA was separated in a 1.2% formaldehyde gel and blotted onto a Hybond N+ membrane (Amersham). Hybridization with <sup>32</sup>P-labeled cDNA probes, labeled by random priming, was carried out as described (20). Expression analysis of the regions flanking the T-DNA insertion in the *AtTBP1* gene was performed, using 2 µg of total RNA and the M-MLV reverse transcriptase RT-PCR kit (Promega) (16). The following primer sets were used: F1 (5'-ATGGTGGTCA AAAGGAAGTTAAATTG-3'), R1 (5'-ACGGGAGTCT TTCGAAAGAAG-3'), R2 (5'-TTCAGAACAAAGAGG TACAGG-3'), R3 (5'-GCGTTGTGAAAGCTCTGTAC G-3'), G1 (5'-GCTTCCCACACAGCTGATCAATTC C-3') specific for the N-terminus; F2 (5'-CAGCACAAA TGAAACAGAACG-3') and R4 (5'-CCATGGTCCTA CCACCAAATTAC-3') for the C-terminus. The relative concentration was evaluated with respect to the reference gene, *60S RP L27A* gene (*At1g70600*). *60S RP L27A* cDNA was amplified with forward (5'-ATGACAACCA GATTCAAGAAGAACAGG-3') and reverse (5'-TTCG GAATACCAAACATTTATCAAATCC-3') primers.

PCR products were resolved by electrophoresis on 1% agarose gels.

### Telomere length analysis

Genomic DNA was extracted from 10-day-old seedlings or individual plant leaves, as described (15). A terminal restriction fragment (TRF) assay was performed with the Tru9I (Promega) restriction enzyme and <sup>32</sup>P 5' end-labeled (CCCTAAA)<sub>7</sub> oligonucleotide as a probe (21,22). Hybridization was done in 0.5 M NaHPO<sub>4</sub> (pH 7.2), 7% SDS, 1 mM EDTA, 1% BSA at 58°C (23). Membranes were washed under the following conditions: low stringency = 2 × SSC, 1% SDS, at 58°C; high stringency = 0.2 × SSC, 0.1% SDS, at 60°C. Single telomere analysis for the right arm of chromosome 2 (Ch2R) was performed, as follows: 10 µl of genomic DNA was digested with PvuII and SpeI, and DNA was separated by electrophoresis in a 0.8% agarose gel and blotted onto a nylon membrane (24). Ch2R telomere-adjacent DNA sequences were amplified with primers Ch2R-F (5'-CTAAACTAGTTGTGTTCCCGTCTCTACT-3') and Ch2R-R (5'-GGTGGGCGACCTTGTGCTTGCCAAA GTC-3') (10).

### Complementation analysis

For the complementation test of *AtTBP1*−/− plants, a 5.1-kb genomic DNA fragment of the *AtTBP1* gene, containing 2.0 kb of putative promoter sequence, was amplified by PCR, using primers TBP1-Compl.-F (5'-GTACCTG CAGTCATGTGTGCACATAGACTATATCAC-3') and TBP1-Compl.-R (5'-GTACCTGCAGTGGCAAAAGTG CAGCAAGCCAAC-3'), cloned into a pGEM-T Easy vector (Promega) and then subcloned into a binary vector pFP100 (25). The complementation vector was introduced into the *Agrobacterium tumefaciens* strain, GV3101. Plants homozygous for the T-DNA disruption in *AtTBP1* were transformed by the *in planta* method (26). Transformants were selected using a seed-expressed fluorescent marker (25) and then genotyped and analyzed for *AtTBP1* mRNA expression and telomere length, as described above.

### Protein expression

Expression of full-length AtTBP1 and AtTBP1-ΔMyb mutant constructs was achieved by using a rabbit reticulocyte lysate TNT system (Promega) under reaction conditions described by the supplier. Briefly, 1.0 µg cloned plasmid DNA was used per 50 µl reaction, containing T7 RNA polymerase in the presence of [<sup>35</sup>S] methionine (to visualize products on SDS-PAGE) or without labeled amino acids (for EMSA). After the transcription-translation reaction, samples were diluted 1:3 with the addition of 100 µl of EMSA buffer. Of this mixture, ~2.0–8.0 µl was used in EMSA reactions.

To test telomeric DNA-binding activity of AtTBP1 mutants, the plant TBP-specific domain deletion mutants were cloned into the vector, pGEX-5X-2, between the EcoRI and XhoI sites, using PCR-generated fragments. GST-AtTBP1<sup>461–640</sup>, ΔC1 (461–592), ΔC2 (461–601), ΔC3 (461–609), ΔC4 (461–618), ΔC5 (461–622) and Δ593–618 were expressed in *E. coli* BL21 (DE3)/RIL cells

(Stratagene) and purified on a GStrap<sup>TM</sup> column, as directed by the manufacturer (Amersham). Mutations R607G and R607I were introduced, using the QuickChange site-directed mutagenesis kit (Stratagene). The protein concentration was determined by Bradford assay and stored in aliquots at  $-80^{\circ}\text{C}$ . Purified proteins were analyzed by SDS-PAGE.

### Electrophoretic mobility shift assay (EMSA)

Electrophoretic mobility shift assay (EMSA) was performed, as described previously (16). Telomeric DNA probes and competitors were designed with double-stranded oligonucleotides. Oligonucleotides were labeled at the 5' end with T4 polynucleotide kinase, using [ $\gamma$ -<sup>32</sup>P]ATP and annealed in TNE buffer (10 mM Tris-HCl, pH 8.0, 100 mM NaCl, 1 mM EDTA) by boiling, followed by cooling to room temperature and purified in 8% polyacrylamide gels. To reduce non-specific DNA-protein binding, proteins were pre-incubated with 1.0  $\mu\text{g}$  poly (dI-dC) in 20  $\mu\text{L}$  EMSA buffer (10 mM Tris-HCl, pH 8.0, 1 mM EDTA, 1 mM dithiothreitol, 50 mM NaCl and 5% glycerol) for 20 min on ice. The end-labeled DNA probe (10 fmol) was added to the reaction mixture. After incubation for 30 min on ice, the mixture was loaded on a 5% non-denaturing polyacrylamide gel (29:1, monomer:bis). Before loading, gels were pre-run at 16 mA for 30 min, and electrophoresis was performed at 16 mA in 1 $\times$  TBE for 2.5 h; dried gels were analyzed using the Phosphorimager (Fuji Photofilm). For competition experiments, varying amounts of cold competitors were pre-incubated with reaction samples before the addition of radiolabeled probe. Binding activity was quantified with an Image Gauge Version 2.53 (Fuji Photofilm).

## RESULTS

### Isolation and characterization of the *AtTBPI* mutant

To study the biological function of *AtTBPI* in *planta*, we screened the INRAV *Arabidopsis* T-DNA insertion collection (19) and identified a putative mutant plant (FST 072C05) with a T-DNA insertion into the *AtTBPI* gene. In the INRAV database, the insertion was annotated within the 10th exon, with the left border oriented toward the 3' end of the *AtTBPI* gene. To determine the genomic organization in detail, including the exact position of insertion, the *AtTBPI*-T-DNA junctions were amplified and sequenced. As shown in Figure 1A, the T-DNA insertion resulted in vast deletion of DNA from the 8th to the 10th exons. We refer to this mutation, which disrupts the gene in the region coding for the conserved DNA-binding motif, as the *attbp1-1* allele. On selective medium, the progeny of self-pollinated heterozygotes segregated in a ratio of  $\sim 3:1$  for the selection marker (Basta-resistant:Basta-sensitive = 467:160;  $\chi^2[1\text{df}] = 0.09$ ). This result suggests that the T-DNA insertion is inherited in a Mendelian manner and indicates a single T-DNA insertion in the *AtTBPI* gene. Southern blot analysis, using T-DNA border sequence as a probe, confirmed that the T-DNA insertion is present at a single locus (supplementary Figure S1).

Northern blot analysis of mutants homozygous for the T-DNA insertion failed to detect *AtTBPI* mRNA, while mRNA of the predicted size,  $\sim 2.5\text{kb}$ , was detected in wild-type plants (Figure 1B). We confirmed that expression of the full-length transcript was abolished by the T-DNA insertion by performing RT-PCR, using various primers. No product was obtained after 38 cycles of PCR amplification (data not shown). RT-PCR of the *AtTBPI* 5' and 3' coding regions flanking the T-DNA insertion, however, revealed the presence of low-abundance transcripts, undetectable by northern blotting (Figure 1C). Remarkably, the expression of an *AtTBPI* mRNA downstream of the insertion was detected (Figure 1C, F2 + R4). As in other T-DNA mutants (11,27,28), these short transcripts are probably abnormal RNA forms that are fused with RNA produced from the T-DNA marker cassette, which is regulated by the 35S promoter and initiated within the T-DNA insert (Figure 1C, L1 + R4). It is unlikely that this unusual RT-PCR product is functional, because it contains only a very short coding region of the C-terminus of *AtTBPI* ( $\sim 30\text{a.a.}$ ). Sequence analysis of the cDNA species, amplified by RT-PCR with the 5' flanking region of T-DNA, predicts that the mutant produces a truncated protein, comprised of the first 451 a.a. of the 640 a.a. full-length *AtTBPI* protein, because a TAA stop codon is encountered in the eighth exon (Figure 1D). These results suggest that the function of this truncated *AtTBPI* protein is severely compromised if not null.

Selected heterozygous plants were self-pollinated to obtain homozygous mutants (G1 *AtTBPI*-/-) and wild-type plants (G1 WT). Four homozygous lines, including two mutant G1 plants and two wild-type plants, were generated from the heterozygous line. These wild-type siblings were used for experimental controls. Individual lines were propagated through successive generations by self-pollination. Seeds from several plants within a single line were pooled each generation until G4. Plants with an *AtTBPI* disruption, however, did not exhibit an obvious phenotypic difference from wild type in the first four generations under normal growth conditions.

### Telomere status in *AtTBPI*-deficient *Arabidopsis*

As *AtTBPI* mutant plants were visibly indistinguishable from wild-type plants, we next examined the role of *AtTBPI* in telomere length homeostasis by determining telomere length in mutant plants with TRF analysis. A recent study suggested that the *Ws* ecotype of *A. thaliana* displays a bimodal size distribution, with one group bearing shorter telomeres (2–5 kb) and the other bearing longer telomeres (4–9 kb) (24). In our experiments, the wild-type telomeres ranged in size from 2.5 to 4.5 kb and were the same size as the telomeres in the short group (Figure 2A, lane 2). This short telomere size of wild-type plants was stably inherited for at least four successive generations (data not shown). In sharp contrast, TRF analysis of G2 to G4 mutant populations showed that telomeres in *AtTBPI* homozygous mutants increased steadily to 10 kb after four generations (Figure 2A, lanes 3–5). Thus, telomeres in *AtTBPI* mutants extended

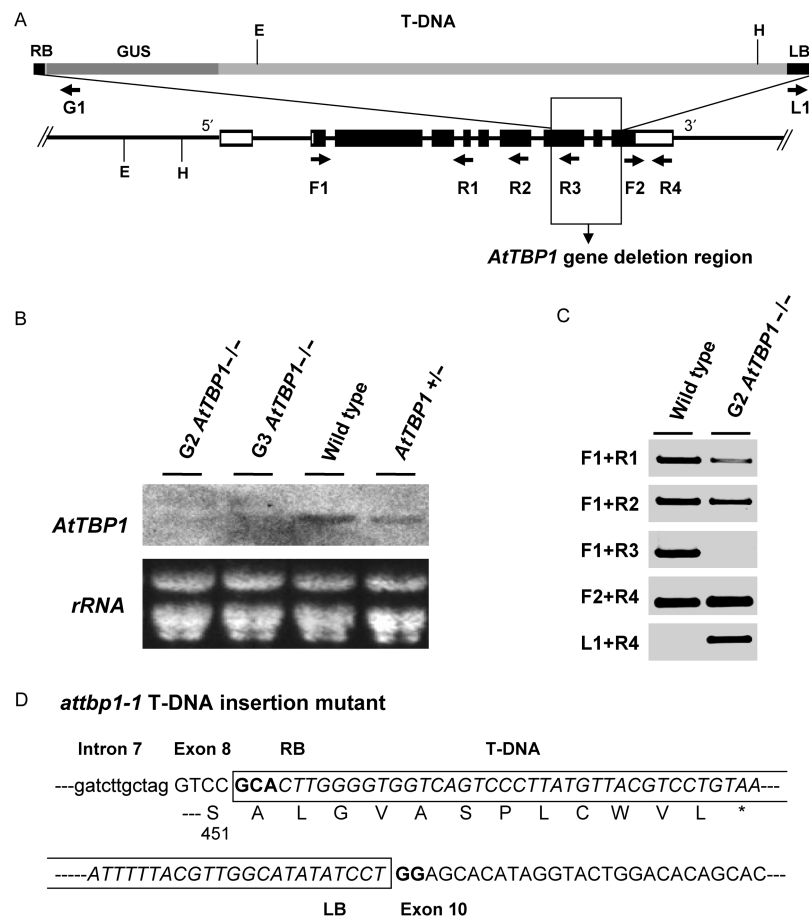


**Figure 1.** Identification of *AtTBP1* T-DNA insertion mutant. (A) Genomic map showing the position of the T-DNA insertion at the *AtTBP1* locus. The arrows indicate the primers used for RT-PCR. Black rectangles represent exons and white rectangles are 5' and 3' UTR regions. E and H represent EcoRI and HindIII restriction sites, respectively. A  $\beta$ -glucuronidase (GUS) cassette was used for DNA-gel blot. LB, left border; RB, right border. (B) Northern blot analysis of *AtTBP1* transcripts in mutant and wild-type plants. Total RNA was hybridized with radiolabeled cDNA corresponding to the *AtTBP1* 5' region (from exon 2 to exon 7). The lower row shows an ethidium bromide staining of rRNA. (C) Analysis of the disrupted *attbp1-1* allele by semi-quantitative RT-PCR. *AtTBP1* transcripts were amplified by 38 cycles of PCR with the indicated sets of primers. (D) The DNA sequence of the junction between the *AtTBP1* cDNA and T-DNA insertion site obtained by RT-PCR. Intron sequences are shown in lowercase letters, and exon sequences are shown in uppercase letters. T-DNA sequences and homologous junction sequences are displayed in italic and boldface uppercase letters, respectively. A translation of the predicted protein is included.

to over twice the size of those in wild-type plants in four generations.

To investigate telomere dynamics in individual plants, we examined TRFs from individual G2 to G4 mutant leaves. As expected, the telomeres in individual mutants increased steadily like those of pooled mutant seedlings (Figure 2B). The banding profile of TRFs in individuals was, however, displayed in a more discrete pattern than that of pooled samples. For analysis of individual chromosome ends, TRF analysis was performed with a probe specific to the Ch2R. As shown in Figure 2C, the Ch2R probe displayed a discrete band of 4–5 kb in wild-type plants, and one or two discrete bands of 4–7 kb in mutant plants. Individual telomere tracts at the same generation were distributed within a 1-kb range. These results indicate that the telomeres in individual mutant plants also increased continuously for each generation.

To verify that the telomere elongation phenotype was associated with the T-DNA insertion in the *AtTBP1* gene,

molecular complementation was performed. A wild-type genomic fragment, containing a putative promoter sequence, was introduced into the *AtTBP1* mutant background via *in planta* transformation. Selected T3 transformants were analyzed for *AtTBP1* mRNA expression and telomere length (Figure 3). The complemented mutants expressed wild-type *AtTBP1* mRNA ectopically (Figure 3A). In each case, the ectopic expression of *AtTBP1* prevented the telomere extension and restored the telomere length to that of the wild-type plants (Figure 3B, lanes 4 and 5). Therefore, we conclude that *attbp1-/-* corresponds to a mutant allele of the *AtTBP1* gene. These results also demonstrate that *AtTBP1* is involved in the regulation of telomere length.

#### Telomeric DNA-binding activity and the functional telomere-binding domain

We previously reported that the isolated C-terminal segment of AtTBP1 is capable of sequence-specific binding

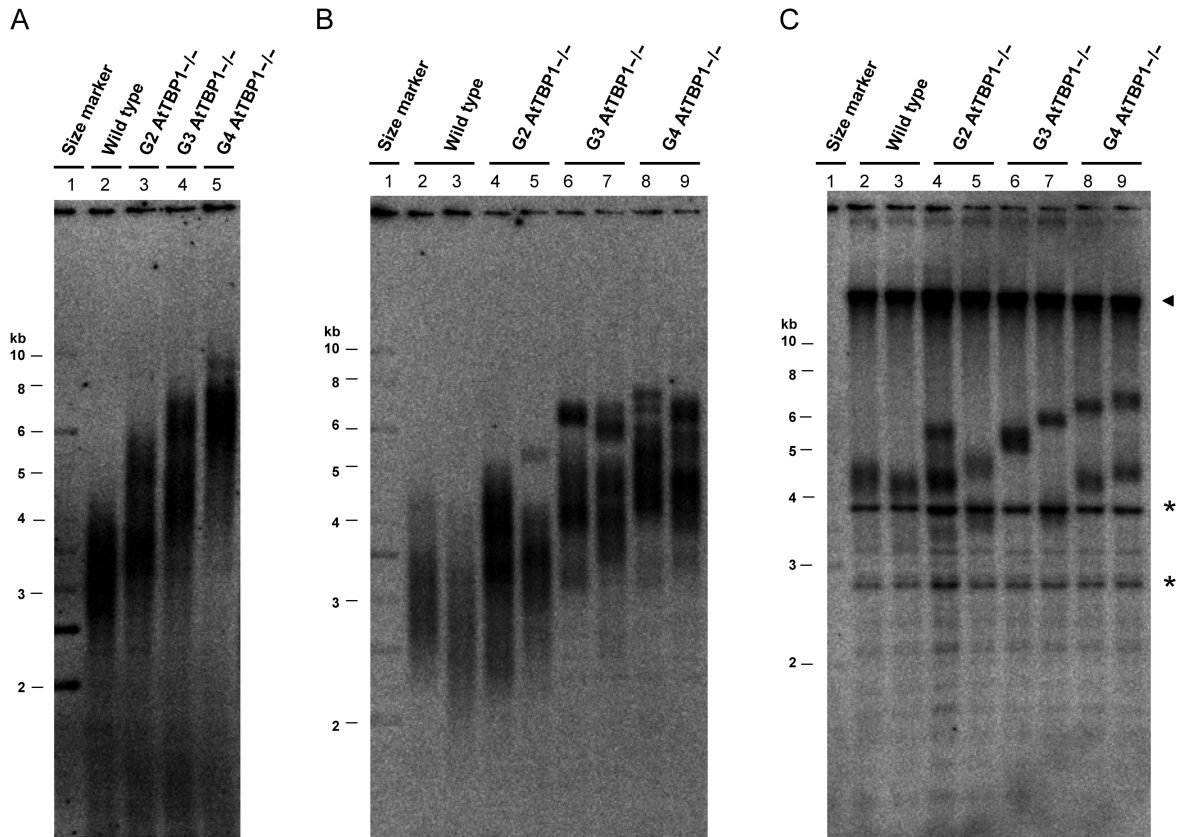


**Figure 2.** Telomere maintenance in *AtTBP1*-deficient plants among different generations. (A) Telomere dynamics in *AtTBP1*<sup>-/-</sup> *A. thaliana*. Genomic DNA isolated from a pool of seedlings of wild type or mutant, at each generation, were digested with Tru9I. Telomeric lengths were determined by Southern hybridization with a telomeric probe. (B) TRF analysis of individual plants from each generation of mutant populations. The gDNAs were extracted from rosette leaves of individual plants and were digested with Tru9I. (C) Single telomere analysis, using a telomere-associated probe derived from the Ch2R. The gDNAs in (C) are the identical samples used in (B), except that these were digested with PvuII and SpeI. The arrowhead indicates undigested gDNAs. The asterisks indicate interstitial telomeric DNA.

to plant telomeric repeats *in vitro* (15,16). The *AtTBP1* mutant that we characterized here, carries a T-DNA insertion at the eighth exon, which encodes the putative DNA-binding domain of *AtTBP1*. Although we could detect no full-length transcripts in *AtTBP1* mutant plants, a transcript of very low abundance, containing the N-terminal sequence upstream of the T-DNA insertion, was detected by RT-PCR. It is unlikely that a truncated protein translated from this RNA would be functional in telomere maintenance. Therefore, we hypothesized that full-length *AtTBP1* binds to plant telomeric DNA, whereas the C-terminal deletion mutant does not bind to plant telomeric DNA. Expression of full-length *AtTBP1* and mutant *AtTBP1* (*AtTBP1*- $\Delta$ Myb) was achieved by using an *in vitro* translation system. As expected, *in vitro* translation of the *AtTBP1* and *AtTBP1*- $\Delta$ Myb cDNAs resulted in the synthesis of a polypeptide with an apparent molecular weight of  $\sim$ 70 and  $\sim$ 50 kDa, respectively (Figure 4A). In order to test whether full-length *AtTBP1* binds to plant telomeric DNA, specifically, the *in vitro* translated protein was used in EMSAs with a radiolabeled DNA probe. The reticulocyte lysate, containing *AtTBP1*, gave rise to a discrete complex, whereas the lysate devoid

of *AtTBP1* did not exhibit any DNA-binding activity under the same conditions (Figure 4B, lanes 2–8). However, the full-length *AtTBP1* and telomeric DNA complexes failed to exit the well of the gel, as also noted from a previous study (29). Nevertheless, the intensities of discrete bands increased upon the addition of an increasing amount of the expressed *AtTBP1* (Figure 4B, lanes 2–4). Competition binding experiments showed that a 5-fold excess of cold *AtTR-4* is enough to displace the labeled probe, whereas higher molar amounts of unrelated non-specific cold competitor (commercial 1-kb DNA ladder marker or non-plant telomeric repeats, such as the human telomeric repeat, TTAGGG) did not compete (Figure 4B, lanes 5–7, data not shown). These results demonstrate that the telomeric DNA-binding activity of full-length *AtTBP1* increased with increasing amounts of protein, and the binding activity was sequence specific to plant telomeric DNA. In contrast, the *AtTBP1*- $\Delta$ Myb mutant did not bind to plant telomeric DNA (Figure 4B, lanes 9 and 10). These results suggest that full-length *AtTBP1* is sufficient for specific interaction with duplex telomeric DNA *in vitro*, and the C-terminus of this protein may be required for the telomeric function

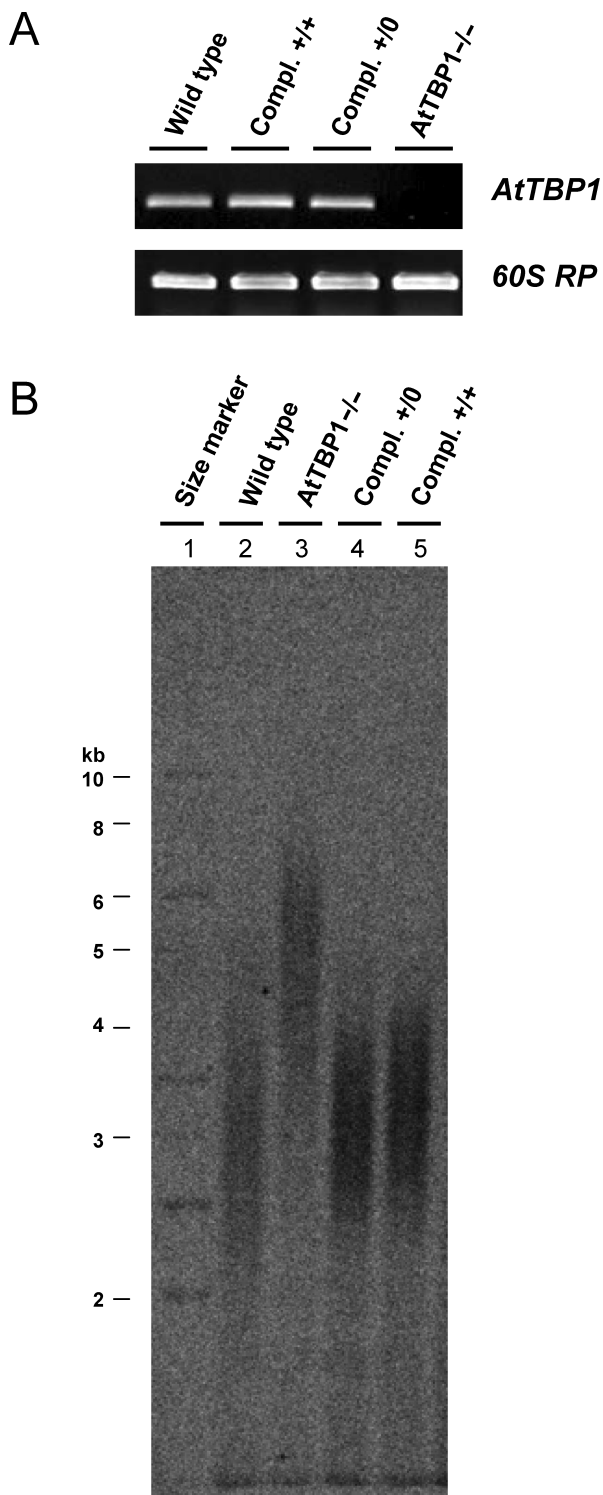


**Figure 3.** Molecular complementation of *AtTBP1* deficiency using wild-type *AtTBP1* gene. (A) Analysis of the complemented plants by semi-quantitative RT-PCR. RNAs of complemented transformants were extracted from seedlings of T3 homozygous and heterozygous plants. *AtTBP1* transcripts were amplified by 35 cycles of PCR with specific sets of primers (F1 and R3). The *60S RP L27A* gene was used to indicate the amount of template for quantitative comparison (bottom panel). (B) TRF assay of complemented plants. Tru9I-digested DNAs from wild-type, *AtTBP1* mutant plants, complemented heterozygous plants (compl.+/0) and complemented homozygous plants (compl.+/+) were analyzed.

of *AtTBP1* *in vivo*. Thus, these results strongly suggest that the telomere length deregulation in the *AtTBP1* mutant may be associated with the loss of the telomeric DNA-binding activity of *AtTBP1*.

Sequence analysis of plant TBPs has demonstrated that there are key features of specific, well-conserved domains (16). Interestingly, plant TBPs have an expanded and plant-specific Myb-domain, which is very highly conserved. We asked whether this domain would play an important role in binding to plant telomeric DNA. Recent results have shown that *A. thaliana* TBPs, TRFL1 (At3g12560) and AtTRP1 (At5g59430), have the Myb-extension domain and that this domain is required for binding plant telomeric DNA (29,30). However, these reports did not characterize the functional region of the Myb-extension domain in detail. Therefore, we characterized several mutant *AtTBP1* proteins in order to define the minimal length for telomeric-DNA binding and also to examine the binding properties of the Myb-extension domain of *AtTBP1*. To examine the contribution of the expanded plant-specific Myb domain and to avoid the problem of protein aggregation associated with the full-length protein-binding assay, we performed EMSA with the various mutated forms, using either fragments or the entire GST-*AtTBP1*<sup>461-640</sup> (Figure 4C). The results shown in Figure 4D demonstrate that the truncated mutants,  $\Delta$ C1 (461-592),  $\Delta$ C2 (461-601), and  $\Delta$ 593-618, did not bind to plant telomeric DNA (lanes 4-7 and lanes 18-20). In contrast, the other mutant proteins,  $\Delta$ C3 (461-609),  $\Delta$ C4 (461-618) and  $\Delta$ C5 (461-622) were capable of binding to the telomeric DNA (lanes 8-13). Lanes 2 and 3 and lanes 12 and 13 showed that  $\Delta$ C5 (461-622) formed a complex with plant telomeric DNA which resembled that of the GST-*AtTBP1*<sup>461-640</sup> control. A noteworthy observation is that, when more of the Myb-extension domain of *AtTBP1* was deleted, weaker DNA-protein complexes were observed (lanes 8 and 9 and lanes 10 and 11). The binding signal of the deletion mutants,  $\Delta$ C3 and  $\Delta$ C4, were 39 and 60%, respectively, of that of GST-*AtTBP1*<sup>461-640</sup> (Figure 4E). Additionally, in order to evaluate the importance of this putative  $\alpha$ -helix portion of the Myb-extension domain, we constructed *AtTBP1* point mutants, containing a glycine (R607G) or an isoleucine (R607I) at position 607. The single substitution of the 607 arginine residue reduced the capacity to bind telomeric DNA to 41% (R607G) and 23% (R607I), respectively, of that of GST-*AtTBP1*<sup>461-640</sup> (Figure 4D lanes 21-26 and Figure 4E). These results firmly support the idea that the region of the plant-specific Myb-extension domain between residues 593 and 622 is critical for optimal plant telomere binding of *AtTBP1*.

A recent study suggested that hTRF1 enters the nucleus through a nuclear import pathway mediated by Importin and that the concentration of nuclear hTRF1 is critical in regulating telomere length (31). Based on these observations, we concluded that understanding the NLS (Nuclear Localization Signal)-singular form of *AtTBP1* should be important in understanding the biological function of *AtTBP1*. In order to confirm the nuclear localization of *AtTBP1*, we performed experiments involving green fluorescent protein fused to *AtTBP1*. Our

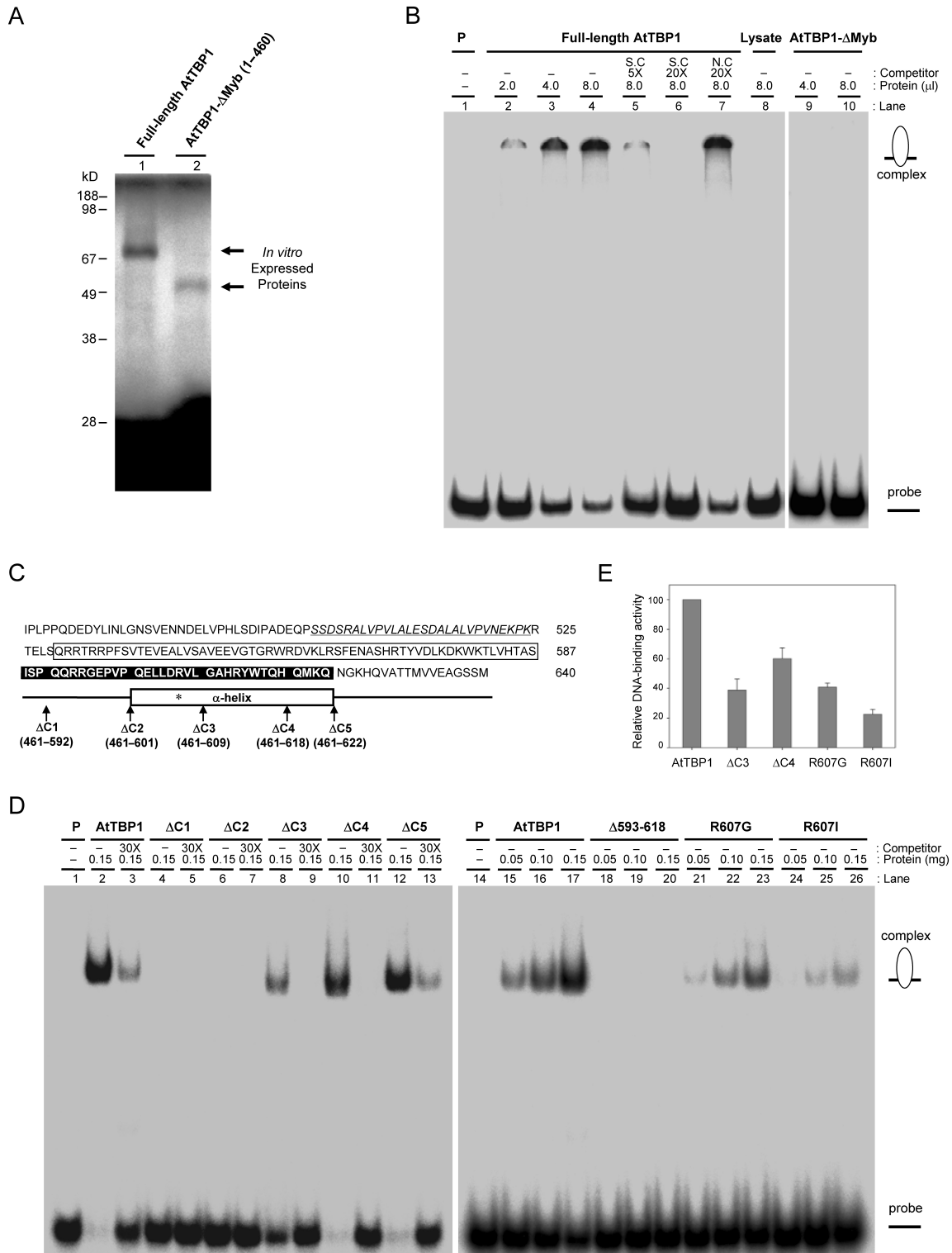


**Figure 4.** DNA-binding properties of full-length AtTBP1 and analysis of Myb-extension domain of AtTBP1. (A) SDS-PAGE gel showing [<sup>35</sup>S] methionine-labeled products resulting from *in vitro* translation of the AtTBP1 derivatives. (B) EMSA with full-length AtTBP1 (lanes 2–7) and AtTBP1-ΔMyb (lanes 9 and 10). The shifted bands indicate DNA–protein complexes with end-labeled plant 4-repeat telomeric DNA (AtTR-4). Schematic diagrams on right-hand sides of figures show possible DNA–protein complexes. (C) Analysis of the Myb-extension domain contained in AtTBP1<sup>461–640</sup>. Domain D (16) is marked with underlined italic letters. The single Myb telomeric DNA-binding domain is indicated with a white box, and the Myb-extension domain is indicated with a black box. The putative α-helix in Myb-extension domain is schematically indicated below. The asterisk indicates the amino acid that was altered by site-directed mutagenesis. (D) DNA-binding properties of Myb-extension domain mutant proteins. EMSA was performed with the various mutant proteins, as shown in (C). The shift bands indicate DNA–protein complexes with end-labeled AtTR-4 in the absence or presence of specific competitor DNAs. (E) Quantification of DNA-binding activities of mutant proteins. The data represent the means of three independent assays; bars denote standard deviation.

localization experiments indicate that AtTBP1 proteins accumulate in nucleus and the NLS for these proteins is present in the fourth basic cluster (287-KRETIHRKRK-296) of the full-length protein (supplementary Figure S2). Thus, these results demonstrate that the functional NLS of AtTBP1 may play crucial roles in telomere functions, such as the localization to the nucleus, in *Arabidopsis*. Because onion cells, in which we transiently expressed GFP-AtTBP1, apparently lack *Arabidopsis*-type telomeric repeats (32), we could not show the sub-nuclear localization of AtTBP1. Therefore, further analysis will be required to determine whether this protein associates specifically with *Arabidopsis*-chromosome ends *in vivo*.

## DISCUSSION

The telomeres of *A. thaliana* became much longer when the *AtTBP1* gene was disrupted. One possible explanation for this phenomenon derives from the roll that shelterins play in telomere length control. Shelterin determines the t-loop architecture of the telomere terminus and controls the synthesis of telomeric DNA by telomerase (1). Disturbing expression levels of shelterin components dramatically impacts on telomere length (1). As t-loops are also observed at plant telomeres (33), the telomere regulation mechanism in *A. thaliana* may be very similar to other eukaryotes. Therefore, the longer telomeres in *AtTBP1* mutant plants could result from a disruption in higher order telomere structure that increases the access of telomerase.

Several mutational analyses revealed that *A. thaliana* telomeric factors are orthologous to human and yeast telomeric factors, but have some unique functions. For example, *AtKu70* mutants have dramatically extended telomeres that reach to ~20–30 kb by the second generation (11,34). Additionally, in *AtKu80*<sup>-/-</sup> cells, telomeres have reached their maximum length (ca. ~10 kb) after 27 weeks, and this length is stable for 34 weeks of growth (12). On the other hand, the telomeres of the *AtTBP1* mutants shown in the present study are like those of *AtMre11* mutants (13), which have telomeres extended to ~10 kb by the fourth generation (Figure 2). These findings demonstrate that these telomeric proteins may have different effects on telomere length. Based on these observations, we suggest that AtTBP1 may have a more subtle role in telomere length regulation, as compared to the double-strand break repair proteins, such as the Ku heterodimer. Recent data showed that *A. thaliana* contains multiple AtTBP1 members which can bind to plant telomeric DNA *in vitro* (16,29), whereas vertebrates have only two double-strand TBPs, TRF1 and TRF2. Thus, it is possible that the plant shelterin structure is more complex than that of human shelterin. Therefore, whether *A. thaliana* plants with mutations in multiple members of this gene family have any effect on telomere homeostasis needs to be investigated further. In addition, monitoring telomere status in subsequent generations of the *AtTBP1* mutants studied in present study will be necessary to determine whether and when equilibrium is reached.

The telomeric-DNA-binding function of AtTBP1 is likely to be completely abolished in the *AtTBP1* mutants, based on our *in vitro* results (Figure 4B). However, we cannot rule out the possibility that a polypeptide derived from the AtTBP1 N-terminus, which was detected at the transcript level by RT-PCR, interferes with the biological functions of the telomere machinery *in planta*. Human TRFs contain different N-terminal domains, such as an acidic domain in hTRF1 and a basic domain in hTRF2, as well as a conserved TRF homology domain, which can form homodimers and also mediate interactions with other telomeric proteins (1). These domains play important roles in protein modification, such as ADP-ribosylation, phosphorylation and ubiquitination, which may play a role in telomere maintenance (35–39). Like other well-known telomere-binding proteins (TBPs), such as hTRF1 and hTRF2, highly conserved domains are also located in the N-terminus of AtTBP1 family members (16,29). Therefore, whether the N-terminal conserved domains of AtTBP1 are involved in metabolism of this protein and/or the regulation of telomere length needs to be investigated further.

One of the most conspicuous differences between AtTBP1 and hTRF1 is the presence of a highly conserved Myb-extension domain in AtTBP1 (Figure 5). We found that the Myb-extension domain is necessary to allow the C-terminus of AtTBP1 to bind to plant telomeric DNA and to stabilize the DNA–protein complex (Figure 4D). The NMR structure of the C-terminus of AtTRP1, which is a member of *A. thaliana* TBPs, displays a novel four-helix tetrahedron rather than the three-helix bundle structure, found in hTRF1 families (30). However, similar to the hTRF1 Myb-domain, AtTRP1 uses a helix-turn-helix motif to bind to telomeric DNA, and the third helix plays a major role in sequence-specific recognition. Although there are structural similarities between plant and animal proteins, our present data showed that Myb-extension domain deletion mutants of AtTBP1, which have an intact, three-helix bundle motif, like hTRF1, were unable to bind either to plant telomeric DNA or to human telomeric DNA *in vitro* (Figure 4D lanes 18–20, data not shown). Therefore, we conclude that the C-terminus of AtTBP1 comprises a domain unique to plants that specifically recognizes plant telomeric DNA.

Taken together, our study provides the first insight into the role of AtTBP1 as a negative regulator of telomere homeostasis in *A. thaliana*. Our results also demonstrate that a plant-specific Myb-extension domain may be critical for recognition of plant telomeric DNA and in stabilization of AtTBP1 binding to plant telomeric DNA. In addition, further analysis of the genetic interactions of AtTBP1 and other telomeric components using previously isolated *A. thaliana* mutants, like *attert*, *atku70*, *atku80*, *atmre11* and others, should help to clarify the contribution of these proteins to telomere maintenance.

## SUPPLEMENTARY DATA

Supplementary Data is available at NAR Online.



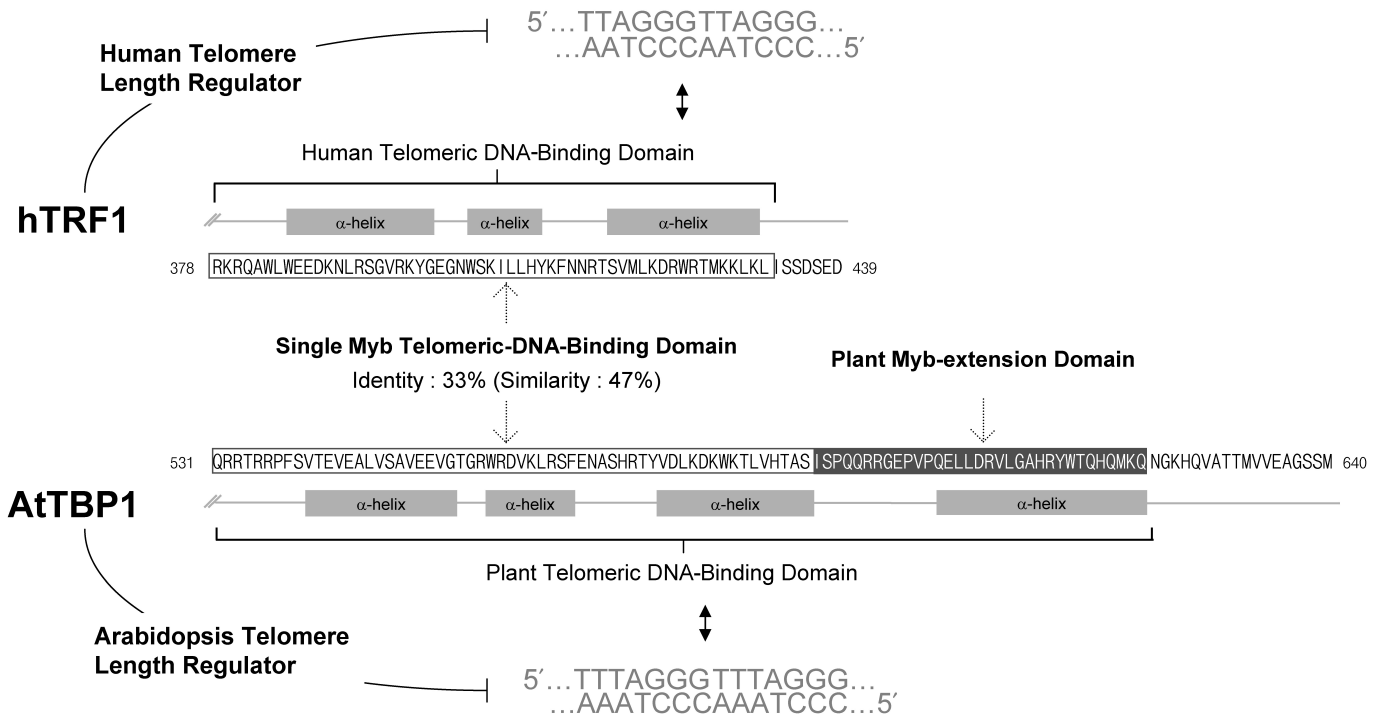


Figure 5. Comparison between AtTBP1 and hTRF1 Myb-domain.

**ACKNOWLEDGEMENTS**

We thank the INRA-FLAG databases for providing the T-DNA knockout resource and François Parcy for his kind gift of the pFP100 vector. This work was supported by grants from the Korean Research Foundation (KRF C00371 and C00438) to M.H.C. Funding to pay the Open Access publication charge was provided by The Second Stage of BK21 (YBRI) of the Ministry of Education of Korea.

*Conflict of interest statement.* None declared.

**REFERENCES**

- de Lange, T. (2005) Shelterin: the protein complex that shapes and safeguards human telomeres. *Genes Dev.*, **19**, 2100–2110.
- Ancelin, K., Brunori, M., Bauwens, S., Koering, C.E., Brun, C., Ricoul, M., Pommier, J.P., Sabatier, L. and Gilson, E. (2002) Targeting assay to study the cis functions of human telomeric proteins: evidence for inhibition of telomerase by TRF1 and for activation of telomere degradation by TRF2. *Mol. Cell. Biol.*, **22**, 3474–3487.
- van Steensel, B. and de Lange, T. (1997) Control of telomere length by the human telomeric protein TRF1. *Nature*, **385**, 740–743.
- van Steensel, B., Smogorzewska, A. and de Lange, T. (1998) TRF2 protects human telomeres from end-to-end fusions. *Cell*, **92**, 401–413.
- Iwano, T., Tachibana, M., Reth, M. and Shinkai, Y. (2004) Importance of TRF1 for functional telomere structure. *J. Biol. Chem.*, **279**, 1442–1448.
- Celli, G.B. and de Lange, T. (2005) DNA processing is not required for ATM-mediated telomere damage response after TRF2 deletion. *Nat. Cell Biol.*, **7**, 712–718.
- Riha, K. and Shippen, D.E. (2003) Telomere structure, function and maintenance in Arabidopsis. *Chromosome Res.*, **11**, 263–275.
- Gallego, M.E. and White, C.I. (2005) DNA repair and recombination functions in Arabidopsis telomere maintenance. *Chromosome Res.*, **13**, 481–491.
- Riha, K., McKnight, T.D., Griffing, L.R. and Shippen, D.E. (2001) Living with genome instability: plant responses to telomere dysfunction. *Science*, **291**, 1797–1800.
- Gallego, M.E. and White, C.I. (2001) RAD50 function is essential for telomere maintenance in Arabidopsis. *Proc. Natl. Acad. Sci. U.S.A.*, **98**, 1711–1716.
- Riha, K., Watson, J.M., Parkey, J. and Shippen, D.E. (2002) Telomere length deregulation and enhanced sensitivity to genotoxic stress in Arabidopsis mutants deficient in Ku70. *EMBO J.*, **21**, 2819–2826.
- Gallego, M.E., Jalut, N. and White, C.I. (2003) Telomerase dependence of telomere lengthening in Ku80 mutant Arabidopsis. *Plant Cell*, **15**, 782–789.
- Bundock, P. and Hooykaas, P. (2002) Severe developmental defects, hypersensitivity to DNA-damaging agents, and lengthened telomeres in Arabidopsis MRE11 mutants. *Plant Cell*, **14**, 2451–2462.
- Ren, S., Johnston, J.S., Shippen, D.E. and McKnight, T.D. (2004) TELOMERASE ACTIVATOR1 induces telomerase activity and potentiates responses to auxin in Arabidopsis. *Plant Cell*, **16**, 2910–2922.
- Hwang, M.G., Chung, I.K., Kang, B.G. and Cho, M.H. (2001) Sequence-specific binding property of Arabidopsis thaliana telomeric DNA binding protein 1 (AtTBP1). *FEBS Lett.*, **503**, 35–40.
- Hwang, M.G., Kim, K., Lee, W.K. and Cho, M.H. (2005) AtTBP2 and AtTRP2 in Arabidopsis encode proteins that bind plant telomeric DNA and induce DNA bending in vitro. *Mol. Genet. Genomics*, **273**, 66–75.
- Karlseder, J., Kachatrian, L., Takai, H., Mercer, K., Hingorani, S., Jacks, T. and de Lange, T. (2003) Targeted deletion reveals an essential function for the telomere length regulator Trf1. *Mol. Cell. Biol.*, **23**, 6533–6541.
- Chiang, Y.J., Kim, S.H., Tessarollo, L., Campisi, J. and Hodes, R.J. (2004) Telomere-associated protein TIN2 is essential for early embryonic development through a telomerase-independent pathway. *Mol. Cell. Biol.*, **24**, 6631–6634.
- Samson, F., Brunaud, V., Balzergue, S., Dubreucq, B., Lepiniec, L., Pelletier, G., Caboche, M. and Lecharny, A. (2002) FLAGdb/FST:

- a database of mapped flanking insertion sites (FSTs) of Arabidopsis thaliana T-DNA transformants. *Nucleic Acids Res.*, **30**, 94–97.
20. Sambrook, J. and Russell, D.W. (2001) *Molecular Cloning: A Laboratory Manual*, 3rd edn. Cold Spring Harbor Laboratory Press, Cold Spring Harbor, NY, USA.
  21. Fitzgerald, M.S., Riha, K., Gao, F., Ren, S., McKnight, T.D. and Shippen, D.E. (1999) Disruption of the telomerase catalytic subunit gene from Arabidopsis inactivates telomerase and leads to a slow loss of telomeric DNA. *Proc. Natl. Acad. Sci. U.S.A.*, **96**, 14813–14818.
  22. Zentgraf, U., Hinderhofer, K. and Kolb, D. (2000) Specific association of a small protein with the telomeric DNA-protein complex during the onset of leaf senescence in Arabidopsis thaliana. *Plant Mol. Biol.*, **42**, 429–438.
  23. Richards, E.J. and Ausubel, F.M. (1988) Isolation of a higher eukaryotic telomere from Arabidopsis thaliana. *Cell*, **53**, 127–136.
  24. Shakirov, E.V. and Shippen, D.E. (2004) Length regulation and dynamics of individual telomere tracts in wild-type Arabidopsis. *Plant Cell*, **16**, 1959–1967.
  25. Bensmihen, S., To, A., Lambert, G., Kroj, T., Giraudat, J. and Parcy, F. (2004) Analysis of an activated ABI5 allele using a new selection method for transgenic Arabidopsis seeds. *FEBS Lett.*, **561**, 127–131.
  26. Clough, S.J. and Bent, A.F. (1998) Floral dip: a simplified method for Agrobacterium-mediated transformation of Arabidopsis thaliana. *Plant J.*, **16**, 735–743.
  27. Puizina, J., Siroky, J., Mokros, P., Schweizer, D. and Riha, K. (2004) Mre11 deficiency in Arabidopsis is associated with chromosomal instability in somatic cells and Spo11-dependent genome fragmentation during meiosis. *Plant Cell*, **16**, 1968–1978.
  28. Mengiste, T., Revenkova, E., Bechtold, N. and Paszkowski, J. (1999) An SMC-like protein is required for efficient homologous recombination in Arabidopsis. *EMBO J.*, **18**, 4505–4512.
  29. Karamysheva, Z.N., Surovtseva, Y.V., Vespa, L., Shakirov, E.V. and Shippen, D.E. (2004) A C-terminal Myb extension domain defines a novel family of double-strand telomeric DNA-binding proteins in Arabidopsis. *J. Biol. Chem.*, **279**, 47799–47807.
  30. Sue, S.C., Hsiao, H.H., Chung, B.C., Cheng, Y.H., Hsueh, K.L., Chen, C.M., Ho, C.H. and Huang, T.H. (2006) Solution structure of the Arabidopsis thaliana telomeric repeat-binding protein DNA binding domain: a new fold with an additional C-terminal helix. *J. Mol. Biol.*, **356**, 72–85.
  31. Forwood, J.K. and Jans, D.A. (2002) Nuclear import pathway of the telomere elongation suppressor TRF1: inhibition by importin alpha. *Biochemistry*, **41**, 9333–9340.
  32. Pich, U. and Schubert, I. (1998) Terminal heterochromatin and alternative telomeric sequences in Allium cepa. *Chromosome Res.*, **6**, 315–321.
  33. Cesare, A.J., Quinney, N., Willcox, S., Subramanian, D. and Griffith, J.D. (2003) Telomere looping in P. sativum (common garden pea). *Plant J.*, **36**, 271–279.
  34. Bundock, P., van Attikum, H. and Hooykaas, P. (2002) Increased telomere length and hypersensitivity to DNA damaging agents in an Arabidopsis KU70 mutant. *Nucleic Acids Res.*, **30**, 3395–3400.
  35. Smith, S., Gariat, I., Schmitt, A. and de Lange, T. (1998) Tankyrase, a poly(ADP-ribose) polymerase at human telomeres. *Science*, **282**, 1484–1487.
  36. Kishi, S., Zhou, X.Z., Ziv, Y., Khoo, C., Hill, D.E., Shiloh, Y. and Lu, K.P. (2001) Telomeric protein Pin2/TRF1 as an important ATM target in response to double strand DNA breaks. *J. Biol. Chem.*, **276**, 29282–29291.
  37. Tanaka, H., Mendonca, M.S., Bradshaw, P.S., Hoelz, D.J., Malkas, L.H., Meyn, M.S. and Gilley, D. (2005) DNA damage-induced phosphorylation of the human telomere-associated protein TRF2. *Proc. Natl. Acad. Sci. U.S.A.*, **102**, 15539–15544.
  38. Chang, W., Dynek, J.N. and Smith, S. (2003) TRF1 is degraded by ubiquitin-mediated proteolysis after release from telomeres. *Genes Dev.*, **17**, 1328–1333.
  39. Lee, T.H., Perrem, K., Harper, J.W., Lu, K.P. and Zhou, X.Z. (2006) The F-box protein FBX4 targets PIN2/TRF1 for ubiquitin-mediated degradation and regulates telomere maintenance. *J. Biol. Chem.*, **281**, 759–768.